Optics & Laser Technology 177 (2024) 111092

Contents lists available at ScienceDirect

Optics and Laser Technology

journal homepage: www.elsevier.com/locate/optlastec

Full length article

Low self-starting threshold polarization-maintaining Er-doped fiber optical frequency comb

Yanwei Gao [a], Haihao Cheng [b], Xiaohong Hu [b], Yongqi Li [a], Hao Liu [a], Yanzhao Yang [c], Ran Pan [b], Yishan Wang [b,*], Shun Wu [a,*]

[a] Hubei Key Laboratory of Optical information and Pattern Recognition, Wuhan Institute of Technology, Wuhan 430205, China
[b] State Key Laboratory of Transient Optics and Photonics, Xi'an Institute of Optics and Precision Mechanics, Chinese Academy of Sciences, Xi'an 710119, China
[c] The 41st Institute of China Electronic Technology Group Corporation, China

ARTICLE INFO

Keywords:
Low self-starting threshold
All-PM figure-9 erbium fiber laser
Optical frequency comb
Polarization-maintaining

ABSTRACT

We report the development of an all-fiber polarization maintaining (PM) optical frequency comb using a mode-locked figure-9 laser with a low self-starting pump threshold. We have achieved self-starting mode-lock for repetition rates (f_r) from 70 MHz to 109 MHz. At a repetition rate of 109 MHz, mode-locking can be achieved for a pump power ranging from 187 mW to 880 mW. To the best of our knowledge, this is the lowest pump power reported for PM figure-9 erbium fiber lasers with repetition rate over 100 MHz. By optimizing the pump power to 238 mW, we have achieved an output power of 5 mW, center wavelength of 1566.2 nm, and 3-dB spectral bandwidth of 20.5 nm. The repetition rate has a high signal-to-noise ratio of 95 dB at a resolution bandwidth of 300 Hz. We have studied the spectral characteristics of the laser under different cavity lengths and pump powers. Additionally, we have stabilized the repetition rate using a GPS-Rb disciplined RF reference. The fractional instability of the repetition rate is measured to be 4.67×10^{-12} at 1 s and 9.22×10^{-13} at 10 s over a measurement of 11 h. Our findings demonstrate that the developed figure-9 comb is robust, compact and has the advantage of high stability and low power consumption. It offers a cost effective solution for future outdoor comb applications.

1. Introduction

The invention of the optical frequency comb [1] has greatly advanced the field of precision metrology [2,3], optical frequency transfer [4], optical atomic clock [5] and astronomical spectroscopy [6–9]. There is a growing demand for outdoor comb applications, which necessitates the development of self-starting polarization-maintaining (PM) fiber combs that offer stable performance, cost efficiency, compactness, and low power consumption. Material-based saturable absorbers (SA) [10–13] such as semiconductor saturable absorber mirrors (SESAM), carbon nanotubes, graphene, topological insulators have been proven to support reliable and self-starting passive mode-locking. However, these materials often have low damage thresholds and degrade over time, making them less desirable.

In comparison, nonlinear amplifying loop mirror (NALM) have several advantages over material-based SAs. They have high damage threshold, fast recovery time, and are cost-effective. All-fiber PM figure-9 lasers based on NALM have emerged as strong contenders for comb oscillator due to their self-starting capabilities and additional benefits of high stability, low noise, and resistance to environmental disturbances [14–19]. However, figure-9 lasers have one major drawback: the mode-locking principle relies on the accumulation of sufficient nonlinear phase differences between the two beams in the NALM cavity. When the repetition rate exceeds 100 MHz, high pump power is usually required to achieve mode-locking.

N. Kuse *et. al.* reported a 83 MHz figure-9 fiber comb in 2016 [20]. The mode-locking is based on a hybrid NALM-SESAM mechanism. In 2020, Yan Pengpeng *et. al.* reported an erbium fiber comb based on NALM with standard deviations of 780 μHz and 308 mHz for repetition rate (f_r) and carrier envelope offset frequency (f_0) locking, respectively [17]. With proper temperature control, Lu Shiyu *et. al.* was able to achieve improved results of 358 μHz for f_r, and 248 mHz for f_0 [19]. However, when the repetition frequency exceeds 100 MHz, the requirement for self-starting pump power becomes stringent. The 121

* Corresponding authors.
E-mail addresses: yshwang@opt.ac.cn (Y. Wang), wushun_wit@163.com (S. Wu).

https://doi.org/10.1016/j.optlastec.2024.111092
Received 10 December 2023; Received in revised form 5 April 2024; Accepted 27 April 2024

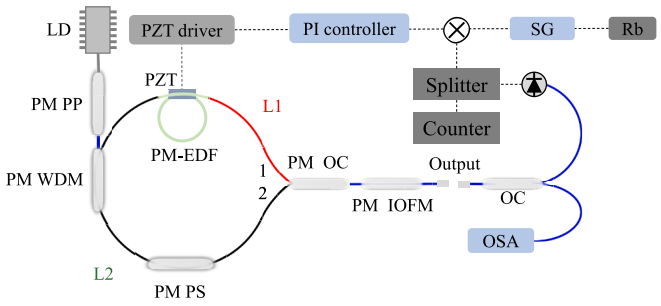

Fig. 1. Experimental setup for PM figure-9 fiber laser comb with repetition rate stabilization. LD: laser diode, PM PP: polarization-maintaining pump protector, EDF: Er-doped fiber, WDM: wavelength division multiplexer, PS: phase shifter, OC: optical coupler with the splitting ratio of 50:50, IOFM: optical fiber mirror and isolator, OSA: optical spectrum analyzer, SG: signal generator, PZT: piezoelectric transducer.

MHz all- PM figure-9 laser reported by Ke Yin et. al. in 2019 has an optimized self-starting pump power of 504 mW for a 18.70 nm spectral bandwidth, and 80 dB signal-to-noise ratio (SNR) of repetition rate [21]. In 2021, Qinghui Deng et. al. proposed a highly compact 201.14 MHz figure-9 laser with only two fiber components in the cavity, which requires 850 mW self-starting pump power [22]. Few references on all-PM figure-9 erbium fiber laser combs have been reported. In 2023, Haihao Cheng *et. al.* reported a 103.4 MHz PM figure-9 laser with a self-starting pump power of 798 mW. The repetition rate is stabilized to Hydrogen maser with a relative frequency stability of 2.1×10^{-12} at 1 s gate time [23]. In the same year, Xinru Cao *et al.* realized a GHz-repetition-rate comb based on a nested fiber ring resonator with a self-starting pump power of 920 mW [24].

In this paper, we mainly discuss the performance optimization and repetition rate stabilization of a PM figure-9 laser. Firstly, we demonstrated an all-PM figure-9 erbium fiber laser with low self-starting pump threshold. In the experiment, mode-locked could be achieved in a repetition rate range from 70 to 109 MHz. We conducted a thorough analysis of the spectral characteristics under different pump conditions and NALM loop asymmetry as repetition rate increased. In particular, we explored how the characteristics of the optical spectrum, such as the central wavelength, the 3 dB bandwidth, and the Kelly sidebands changed with 1) pump power and 2) loop asymmetry for various repetition rates below and around 100 MHz. We observed that increasing in the NALM loop asymmetry effectively reduced the self-starting and mode-locking pump thresholds, as demonstrated in the Ref. [25]. To the best of our knowledge, among the published literatures on all-PM figure-9 erbium lasers with repetition rate over 100 MHz, our laser has the lowest self-starting pump threshold power for mode-locking. Secondly, with repetition rate stabilized to a GPS-disciplined Rb oscillator, our comb demonstrates stable operation for more than 11 h without temperature control. The fractional instability was measured to be 4.67×10^{-12} and 9.22×10^{-13} at 1 s and 10 s sampling time, respectively. This result is comparable to that stabilized to hydrogen maser in Ref. [23]. With additional temperature control, it is expected to achieve days even months of stable operation. This self-starting figure-9 comb has low self-staring threshold and high stability, laying a good foundation for further study of figure-9 combs. Additionally, the compact structure of the all-PM fiber comb is conducive to miniaturization development.

2. Experiment setup

Fig. 1 illustrates the experimental setup of an all-PM fiber comb based on a figure-9 laser. The laser consisted of a 980-nm laser diode (LD), an NALM loop, and a linear cavity. In the NALM loop, a 32 cm PM EDF (Liekki, Er80-4/125-HD-PM) was pumped by a 976 nm LD through

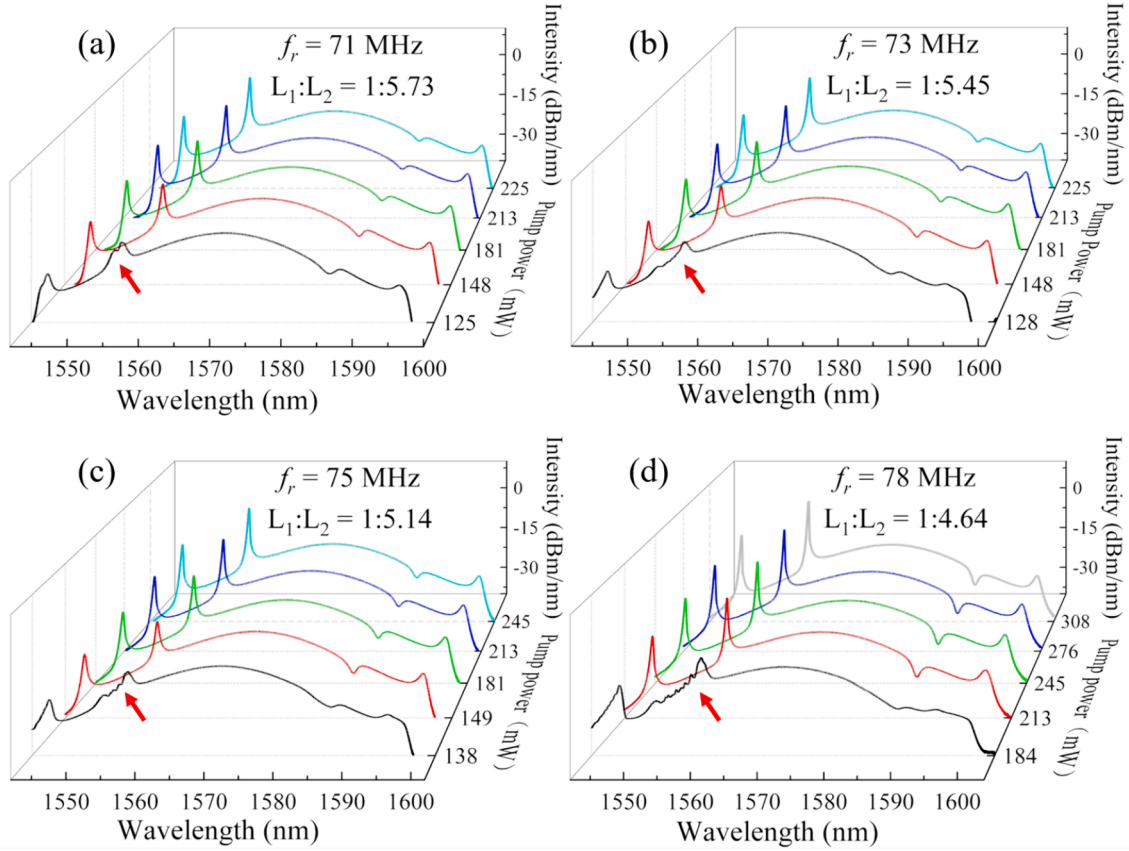

Fig. 2. Output spectra of the laser under different pump power and repetition rate when the length of the EDF is 36.4 cm.

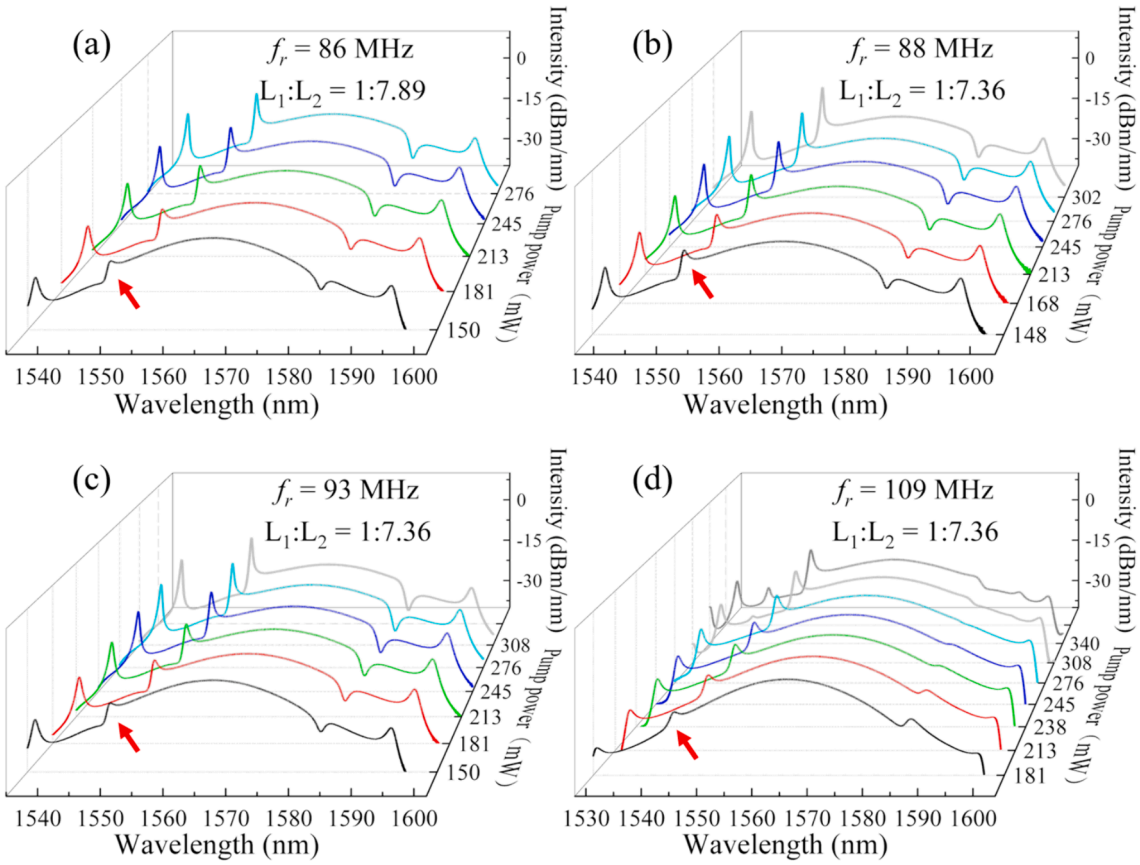

Fig. 3. Output spectra of the laser under different pump power and repetition rate when the length of EDF is 32.1 cm.

a WDM. A $\pi/2$ phase-shifter (PS) was used to help the laser mode-locking and reduce the mode-locking threshold. The linear cavity of the laser was an optical fiber mirror with isolation, which was used to form a resonant cavity and output laser pulses. The NALM loop and the linear cavity were connected by a 50/50 output coupler, which was used to accumulate appropriate phase bias between the clockwise and counterclockwise beams. The net cavity dispersion was about $-0.023\ ps^2$. The total cavity length of the laser was 182 cm, corresponding to a repetition rate of 109 MHz. To control the cavity length, the erbium fiber was wounded twice before it was glued to a PZT stretcher to compensate for any variations caused by environmental disturbances. We chose to place PZT on EDF because it was the longest fiber in the laser cavity and was least likely to cut short during the optimization process. The output of the laser was received by a photodetector. The generated repetition rate signal was mixed with the GPS-Rb reference and produced the error signal. The output voltage was fed back to the PZT in the laser cavity through RF filtering and amplification for a stable repetition rate locking.

3. Result and discussion

In this section, we focuses on the optimization characteristics and stabilization results of the figure-9 laser. We investigate the laser optimization characteristics in three aspects. Firstly, we analyze the evolution of the optical spectrum under different pump conditions and NALM loop asymmetry as the repetition rate increases from 71 to 109 MHz. We observed how the NALM loop asymmetry affects the Kelly sideband behavior in the optical spectrum. Additionally, as the repetition frequency changes from 78 to 86 MHz, we find that increasing the loop asymmetry is beneficial for obtaining a lower threshold pump power, while the self-starting threshold differs by only a few mW. We present the output characteristics of the laser at the optimized repetition rate of 109 MHz. Secondly, we measure the repetition rate shift, power and output spectrum stability of the laser oscillator during free operation. Finally, we measure the frequency fractional instability of the repetition rate when it is locked to the GPS-Rb oscillator.

3.1. The figure-9 laser performance

During the optimizing process, we investigate how the optical spectrum evolves under different pump conditions and NALM loop asymmetry for different repetition rates. The NALM loop's asymmetry is determined by the length ratio, L_1/L_2, where L_1 is the counter-clockwise distance from the output coupler's port 1 to the EDF (red portion in Fig. 1), and L_2 is the distance from the output coupler to the phase-shifter and then the EDF (black portion). It is common for the peak power of the Kelly sidebands to decrease when the pump power is reduced. However, we observed that the change in the Kelly sidebands is also related to the NALM loop's asymmetry. Fig. 2 illustrates the optical spectrum of the laser oscillator under various pump conditions when L_1 is 22.6 cm, and the asymmetry ratio (L_1/L_2) is 1:5.73, 1:5.45, 1:5.14, and 1:4.64, respectively. All the repetition rates are around 75 MHz for comparison. Kelly sidebands in the form of spectral peaks and dips were both shown in the spectrum. The formation of Kelly sidebands is as follows: Optical solitons experiences periodic gain and loss in the oscillator. In order to maintain their own stability, dispersion waves will be emitted when the disturbed solitons are restored, which will interact with the soliton during the process of transmission in the fiber cavity. When the dispersive wave is in phase with the soliton at a certain position in the cavity, a local instructive interference is formed, which is manifested as a peak sideband. On the contrary, if the two are out of phase, destructive interference is formed, shown as the dip sidebands at around 1585 nm in Fig. 2. We made two important observations: Firstly,

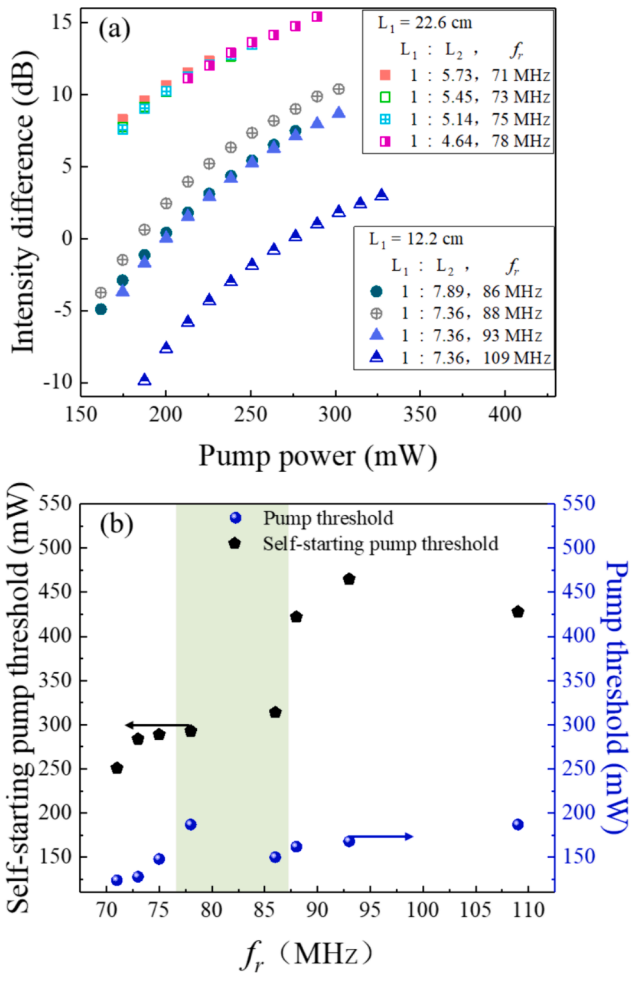

Fig. 4. The effect of loop asymmetry. (a) The relationship between the optical intensity difference between the peak of mode-locked spectrum and the Kelly sideband as a function of the pump power. (b) Self-starting and mode-locked pump thresholds at different repetition rates (or different loop asymmetry).

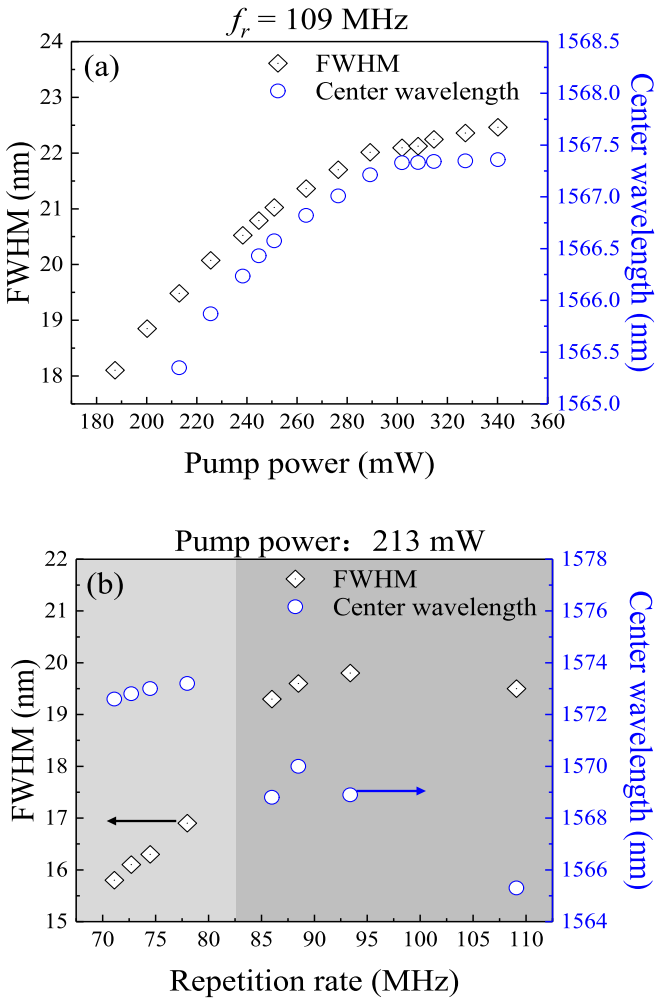

Fig. 5. The variation of spectral chatericticsin Figs. 2 and 3. (a) The spectral width and central wavelength as a function of pump powers when the repetition frequency is 109 MHz. (b) The spectral width and central wavelength of the same pump power as a function of repetition rates.

when the pump power was reduced below 190 mW, small ripples showed up near the Kelly sidebands at the short-wavelength end of the spectrum, as shown in black curves in Fig. 2. Secondly, although the peak power of the Kelly sidebands was reduced as pump decreases in all cases, it remained higher than the peak power of the mode-lock spectrum. In all four cases, the net cavity dispersion was between −0.043 and −0.037 ps^2.

Based on the analysis in Fig. 2, we further increased the loop asymmetry to 1:7.89 until we obtained the result that the intensity of the highest Kelly sideband was lower than that of the center wavelength, as shown Fig. 3(a). Fig. 3 (b-d) studied the spectral performance when the repetition frequency was increased from 88 MHz to 109 MHz by reducing the length of the linear cavity. In all the three cases, L_1 was set to be 12.2 cm, and the asymmetry of the loop cavity remained the same (1:7.36). Compared to Fig. 2, we noticed that when the pump power was reduced to less than 190 mW, all the spectrum in Fig. 3 were very smooth, as indicated by the red arrows. Moreover, the pump power control suppressed the peak power of the Kelly sidebands better than in Fig. 2. The net cavity dispersion in Fig. 3 was between −0.034 and −0.023 ps^2.

According to Ref [26], the power of the first-order Kelly sidebands was significantly influenced by two factors inside the laser cavity: the total dispersion D and the nonlinear coefficient δ. When the total dispersion D is negative and close to zero, the effect of D on Kelly sidebands is relatively small compared to that of the nonlinear coefficient δ [26]. When increasing the repetition frequency from 88 MHz to 109 MHz, the nonlinear coefficient related to the length and Kerr coefficient of the fiber is reduced as the cavity length decreases. The overall change in the cavity dispersion is only 0.02 ps^2. Therefore, the Kelly sideband light intensity decreases. In addition, Ref [25] asserted that the larger the coupler splitting ratio, the higher the mode-locking threshold would be. Therefore, the 50/50 coupler in our laser configuration is expected to obtain the lowest mode-locking threshold. For a fixed coupler splitting ratio, the loop asymmetry can be optimized for a large self-start single-pulse mode-locking region [25], and thus the mode-locking threshold can be reduced.

To study the influences of loop asymmetry on the optical spectrum, we investigated how the peak intensity of the Kelly sideband varies relative to that of the mode-lock spectrum. Fig. 4(a) plots the optical intensity differences under various conditions, including pump power, loop asymmetry ratio, and repetition rates. The overall trend we observed was that the Kelly sideband can be suppressed as the pump power decreases, and that the asymmetry ratio and repetition rate also played a vital role in this process. By working in a proper asymmetry ratio range and with repetition rates close to 100 MHz, it is possible to effectively reduce the Kelly sideband. As the repetition frequency increases, the cavity length decreases, leading to a reduction in the nonlinear coefficient related to the length and the Kerr coefficient of the fiber. At this time, the total dispersion in the cavity is negative near zero.

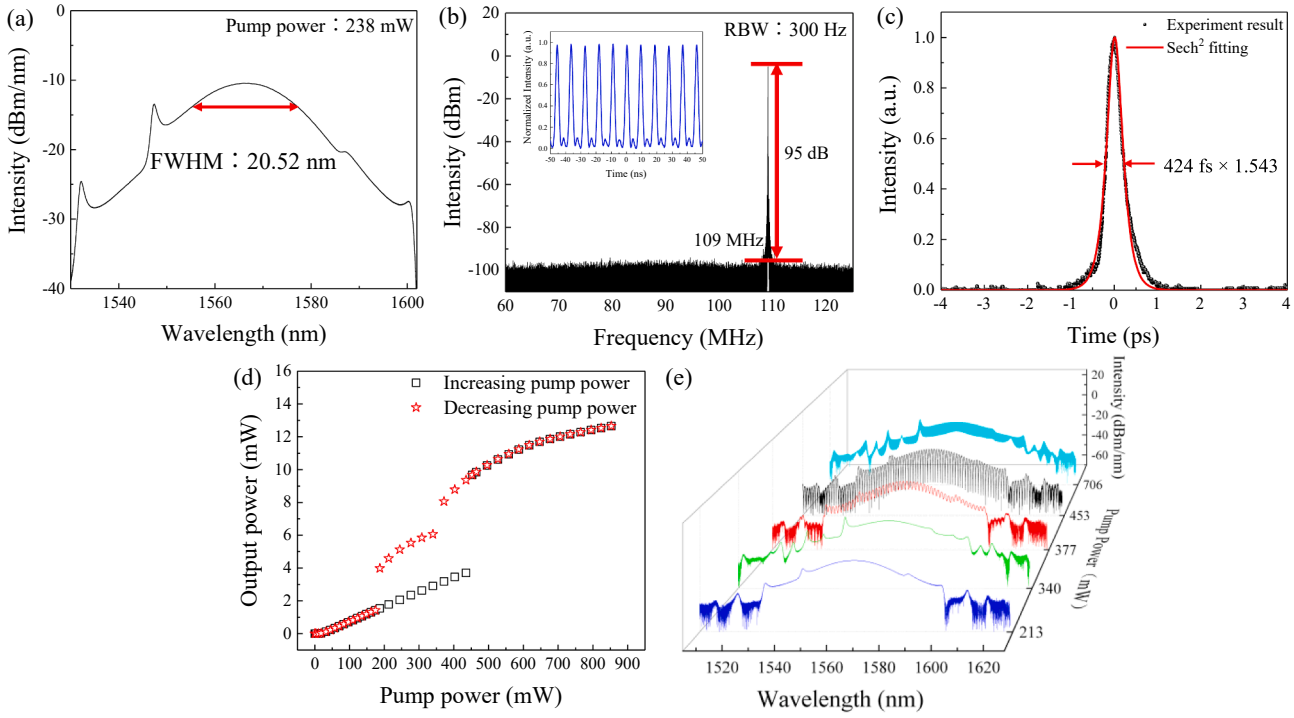

Fig. 6. The optimized output characterization of the laser. (a) Optical spectrum at a pump power of 238 mW. (b) The measured RF spectrum showing the repetition frequency. Inset: The time domain pulse trains measured by a 2 GHz oscilloscope. (c) The intensity autocorrelation trace of the output pulse from the oscillator after 0.75 m PM 1550 fiber. (d)The output average power as a function of pump power. (e) The optical spectrum evolution under different pump powers.

Therefore, when the loop asymmetry is increased, the intensity of the Kelly sideband light is significantly reduced due to the decrease of the nonlinear coefficient and the total dispersion [26]. In Fig. 4, it can be seen that increasing the asymmetry of the loop from 1:4.64 (L_1 = 22.6 cm) to 1:7.89 (L_1 = 12.2 cm), or changing the repetition rate from 78 MHz to 86 MHz, does not significantly affect the self-starting threshold pump of the laser, but lowers the mode-locking pump threshold. This is because a larger loop asymmetry helps to accelerate the accumulation of nonlinear phase, which is beneficial for reducing the mode-locking pump thresholds. By adjusting the loop asymmetry and combining it with a phase shifter, it is possible to achieve low self-starting and mode-locking thresholds. These findings are consistent with the point mentioned in Ref.[25], although they only considered the effect of loop asymmetry on the two threshold powers under the same repetition rate, while we observed that under various repetition rate conditions. With increasing repetition rate, sufficient nonlinear phase shift must be accumulated to achieve self-starting mode locking, which can be compensated by increasing the pump power to make up for the reduction in cavity length. The experimental results in Fig. 4 (b) confirmed this point. For all the measurements, the net cavity dispersion was similar, which was around $-0.03 \pm 0.01\ ps^2$.

To study how the spectral characteristics were influenced by the loop asymmetry and pump power, we recorded and plotted the changes of spectral width and central wavelength in Fig. 5. As pump power increases, the spectral width gradually widens from 18 nm to 22 nm for a repetition rate of 109 MHz, while the central wavelength exhibits red shift from 1565.3 nm to 1567.4 nm, illustrated in Fig. 5(a). In Fig. 5(b), with the increase of repetition rate from 70 MHz to 109 MHz, the spectral width increases from 15.8 nm to almost 20 nm at a constant pump power of 213 mW, while the central wavelength shows blue shift by over 8 nm. However, we observed that there is a region where spectral distortion is prone to occur, indicated by the red arrows in Fig. 2, when adjusting the length of L_2. This region, colored in light grey in Fig. 5(b), leads to unstable RF spectrum and time domain waveform. In contrast, stable spectrum and time domain waveform were obtained when the EDF was 32.1 cm, represented by the dark grey region on the right.

Moving to Fig. 6, we present the output characteristics of the mode-locked figure-9 laser at an optimized pump power of 238 mW. The Kelly sidebands were successfully suppressed below the mode-lock spectrum. The spectrum was centered at 1566.2 nm with a 3-dB spectral bandwidth of 20.5 nm. The RF spectrum of the 109 MHz repetition rate is represented in Fig. 6(b). The inset picture shows the pulse train recorded by a 2 GHz oscilloscope. We measured the pulse width using an intensity

Table 1
PM Erbium-doped mode-locked fiber laser with repetition rate above 100 MHz.

EDF length (cm)	f_r(MHz)	Self-starting threshord pump power (mW)	Pump power[a] (mW)	FWHM (nm)	λ_c(nm)	Output power (mW)	NCD (ps^2)	Refs.
–	907	920	–	15.5	1530	4.5	–	[24]
31	201	850	–	20.9	1561.3	4	−0.0124	[22]
35	121	504	504	18.7	1571.6	1.2	−0.015	[21]
28	103.4	798	460	20.6	1562	6.82	−0.02	[23]
32.1	109	428	238	20.5	1566.2	5	−0.023	Our
32.1	109	428	187	18.1	1563.8	4	−0.023	work

[a]The pump power is the set power of laser data acquisition.

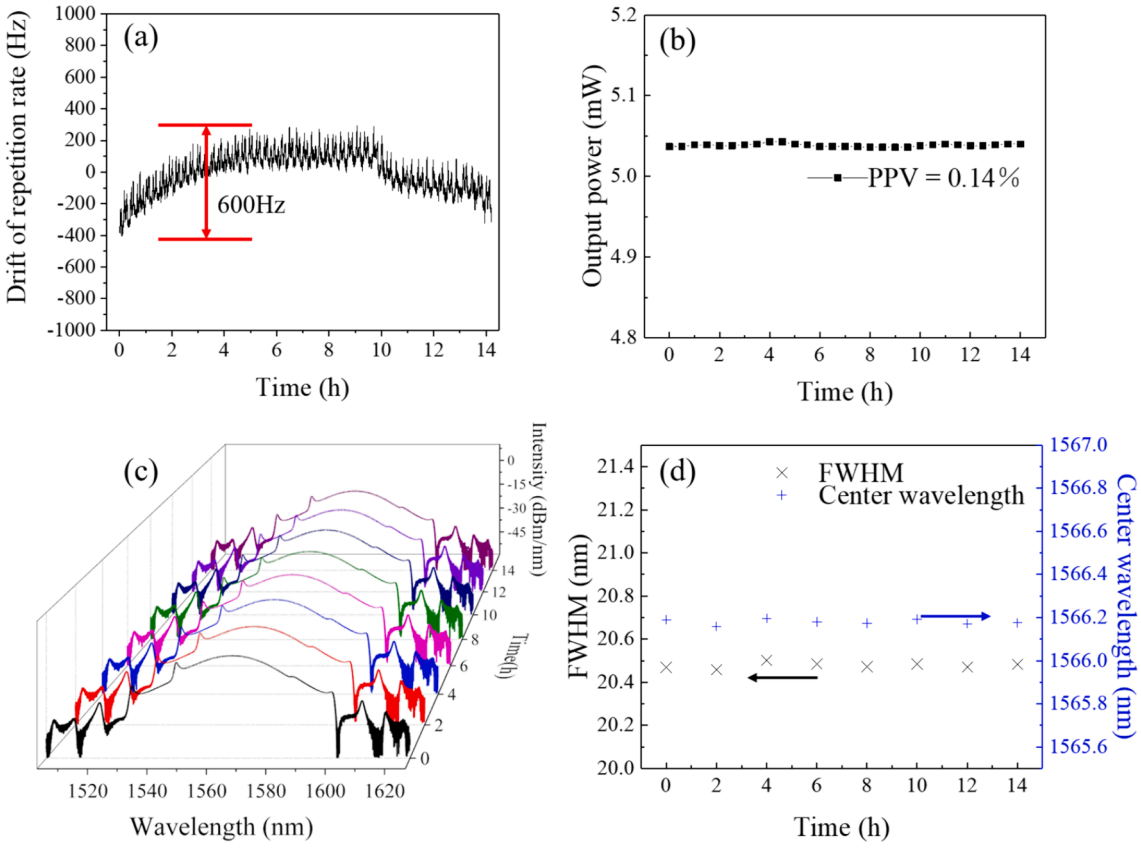

Fig. 7. The 14- hour stability test for the laser. (a) Free running drift of repetition frequency; (b) Output power; (c) Optical spectrum; (d) 3 dB spectral width and central wavelength of the laser.

autocorrelator (Feomto-chrome, FR-103XL) based on second-harmonic generation (SHG). Fig. 6(c) illustrated the autocorrelation measurement of the oscillator output after 0.75 m PM1550 fiber. By fitting the $sech^2$ function, the pulse duration was measured to be 424 fs. The time-bandwidth product was calculated as 1.064. Fig. 6(d) plotted the output power of the laser. As the pump power increased, the laser remained cw lasing until the pump reached the self-staring threshold of 428 mW. The spectrum exhibited bound-state mode-locking with an output power of around 10 mW. However, when we reduced the pump power below 352 mW, the spectrum jumped from bound-state mode-locking to single pulse mode-locking, as shown in Fig. 6(e).

Table 1 lists several published work in recent years on all-PM figure-9 erbium fiber lasers and combs with repetition rates above 100 MHz. Among them, our comb exhibited the lowest mode-lock self-staring pump threshold (428 mW) with about the same EDF length and lowest working pump power. Similar spectral width and output power are obtained when the pump power is reduced to 187 mW.

3.2. *The stability of free-running figure-9 Er:laser*

We monitored the repetition rate, output power and optical spectrum of the laser for 14 h in an air-conditioned laboratory, as shown in Fig. 7. In Fig. 7(a), the drift of repetition rate was about 600 Hz. The output optical power was measured every half an hour, and showed a power fluctuation of 0.14 %. Fig. 7(c-d) plotted the spectral repeatability over a span of 14 h.

3.3. *Frequency fractional instability of figure-9 Er:laser*

We stabilized the repetition frequency to a frequency synthesizer and measured the fractional instability. This was achieved by mixing the fundamental repetition rate with the reference signal from the synthesizer to generate an error signal. The error signal was filtered and amplified through the PI controller. The output of the PI controller was fed back to the PZT driver for precise cavity length control. Fig. 8(a) represented the repetition frequency recorded by the Keysight frequency counter (Model No.:53230A) at a gate time of 1 s for over 11 h. Both the frequency counter and the RF reference signal are using the GPS-disciplined Rb oscillator as reference. The red triangles and green **square** in Fig. 8(c) represented the instability of the GPS-Rb oscillator, and the synthesizer which was referenced to the GPS-Rb oscillator, respectively. The measured Allan deviation of the repetition frequency was 0.5 mHz. The fractional instability at 1 s and 10 s sampling time was 4.67×10^{-12} and 9.22×10^{-13}, respectively, represented by the blue dots ~~in~~ ~~(b)~~, which followed the synthesizer performance as expected. Currently, the experiments were conducted in an air-conditioned laboratory. The long-term stability of the system can be further enhanced in future with the help of additional temperature control for the laser oscillator.

4. Conclusion

In this paper, we have constructed an all-PM fiber laser optical frequency comb based on figure-9 erbium fiber laser with 428 mW self-starting pump threshold and fractional stability on the order of 10^{-13} at 100 s gate time. As far as we know, this is the lowest self-starting pump threshold reported for all-PM figure-9 erbium fiber comb with repetition rate above 100 MHz. Through our research, we have discovered that the NALM loop asymmetry plays a crucial role in achieving a low self-starting threshold. By studying the position of the gain fiber, we have optimized the asymmetry of the loop cavity, allowing for a low operating pump power of 187 mW with a 50/50 coupling ratio and 109 MHz repetition frequency. The repetition

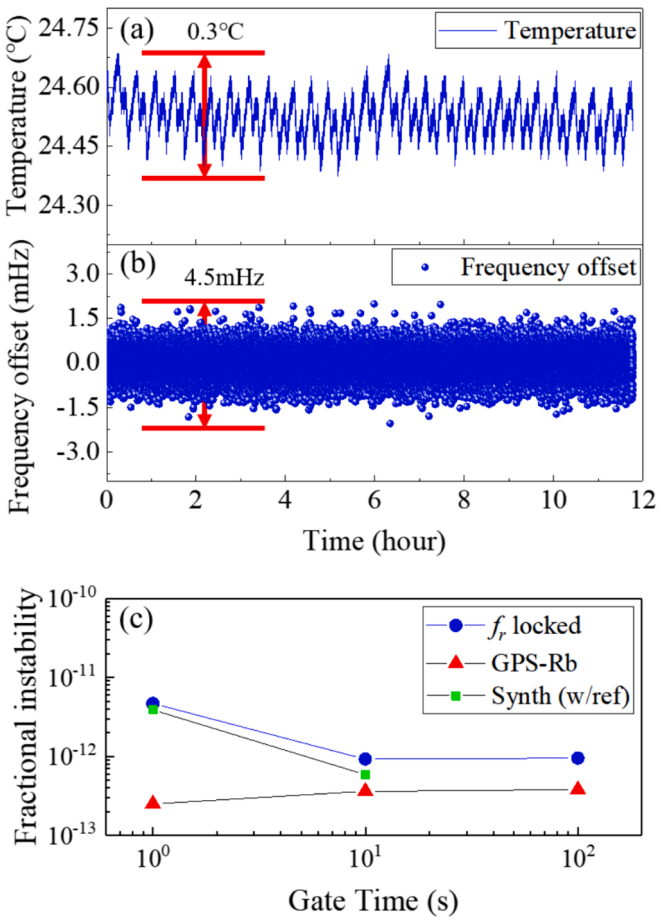

Fig. 8. Repetition rate locking results. (a) Room temperature variation during the measurement. (b) Stabilized repetition rate for over 11 h at 1 s gate time. (c) The fractional instability of repetition rate (blue dots), the RF synthesizer when referenced to the GPS-Rb oscillator (green square), and the GPS-Rb oscillator (red triangle).

frequency of the laser was currently limited by the minimum length for fiber splicing. If we could combine phase shifter, WDM and output coupler to a single device, the repetition frequency can be enhanced to more than 200 MHz.

Furthermore, we analyzed the changes of spectral properties, such as the center wavelength and spectral width, for different NALM loop asymmetries and pump powers as the repetition rate increases. Our results have shown that the NALM loop asymmetry not only played a crucial role in achieving a low self-starting threshold, but also significantly affects the intensity of the spectral Kelly sidebands. By selecting an appropriate asymmetry, we were able to greatly suppress the Kelly sideband. Additionally, our reproducibility test over a span of 14 h also validated the long-time stable operation in terms of output power and spectral shape.

Moreover, we have achieved frequency stabilization of the repetition rate locking for over 11 h, attaining a fractional instability was 4.67×10^{-12} and 9.22×10^{-13} for at 1 s and 10 s gate time, respectively. This stability can be further enhanced through improved isolation and external temperature control. We believe that the compact and robust frequency comb presented in this paper holds immense potential in becoming a highly promising ultrafast fiber comb source in the fields of precision measurement, optical sensing, optical communication, lidar, and other outdoor applications.

CRediT authorship contribution statement

Yanwei Gao: Writing – original draft, Visualization, Validation, Investigation, Formal analysis, Data curation, Conceptualization. **Haihao Cheng:** Data curation. **Xiaohong Hu:** Data curation. **Yongqi Li:** Investigation. **Hao Liu:** Investigation. **Yanzhao Yang:** Resources. **Ran Pan:** Resources. **Yishan Wang:** Resources. **Shun Wu:** Writing – review & editing, Validation, Supervision, Funding acquisition, Conceptualization.

Declaration of competing interest

The authors declare that they have no known competing financial interests or personal relationships that could have appeared to influence the work reported in this paper.

Data availability

Data will be made available on request.

Acknowledgements

The authors acknowledge the funding from the Campus Science Foundation of Wuhan Institute of Technology [grant number 22QD01], the Open Research Fund of State Key Laboratory of Transient Optics and Photonics (No. SKLST202105), and the Natural Science Foundation of Hubei Province of China (No. 2023AFB778).

The authors also acknowledge Prof. Chenggang Guan in the School of Science, Hubei University of Technology for the generosity of sharing equipment with us for this work.

References

[1] J.L. Hall, Nobel Lecture: Defining and measuring optical frequencies, Rev. Mod. Phys. 78 (2006) 1279–1295, https://doi.org/10.1103/RevModPhys.78.1279.
[2] A. Cingöz, D.C. Yost, T.K. Allison, A. Ruehl, M.E. Fermann, I. Hartl, J. Ye, Direct frequency comb spectroscopy in the extreme ultraviolet, Nature 482 (2012) 68–71, https://doi.org/10.1038/nature10711.
[3] B. Xu, X. Fan, S. Wang, Z. He, State Key Laboratory of Advanced Optical Communication Systems and Networks, Department of Electronic Engineering, Shanghai Jiao Tong University, Shanghai 200240, China, Sub-Femtometer-Resolution Absolute Spectroscopy with Sweeping Electro-Optic Combs, OEA 5 (2022) 210023, https://doi.org/10.29026/oea.2022.210023.
[4] S. Zhang, J. Zhao, Frequency comb-based multiple-access ultrastable frequency dissemination with 7 × 10 - 17 instability, (n.d.).
[5] J. Yao, J. Sherman, T. Fortier, H. Leopardi, T. Parker, J. Levine, J. Savory, S. Romisch, W. McGrew, X. Zhang, D. Nicolodi, R. Fasano, S. Schäffer, K. Beloy, A. Ludlow, Progress on optical-clock-based time scale at NIST: Simulations and preliminary real-data analysis: Optical-Clock-Based Time Scale at NIST, NAVIGATION 65 (2018) 601–608, https://doi.org/10.1002/navi.248.
[6] C.-H. Li, A.G. Glenday, D.F. Phillips, G. Furesz, N. Langellier, M. Webber, A. Zibrov, A.J. Benedick, G. Chang, L.-J. Chen, D. Sasselov, F. Kärtner, A. Szentgyorgyi, R.L. Walsworth, Green astro-comb for HARPS-N, in: I.S. McLean, S.K. Ramsay, H. Takami (Eds.), Amsterdam, Netherlands, 2012: p. 84468X. doi: 10.1117/12.925799.
[7] T. Wilken, G.L. Curto, R.A. Probst, T. Steinmetz, A. Manescau, L. Pasquini, J. I. González Hernández, R. Rebolo, T.W. Hänsch, T. Udem, R. Holzwarth, A spectrograph for exoplanet observations calibrated at the centimetre-per-second level, Nature 485 (2012) 611–614, https://doi.org/10.1038/nature11092.
[8] T. Herr, R.A. McCracken, Astrocombs: Recent Advances, IEEE Photon. Technol. Lett. 31 (2019) 1890–1893, https://doi.org/10.1109/LPT.2019.2950528.
[9] R. Yang, M. Zhao, X. Jin, Q. Li, Z. Chen, A. Wang, Z. Zhang, Attosecond timing jitter from high repetition rate femtosecond "solid-state fiber lasers", Optica 9 (2022) 874, https://doi.org/10.1364/OPTICA.457835.
[10] Y. Feng, X. Xu, X. Hu, Y. Liu, Y. Wang, W. Zhang, Z. Yang, L. Duan, W. Zhao, Z. Cheng, Environmental-adaptability analysis of an all polarization-maintaining fiber-based optical frequency comb, Opt. Express 23 (2015) 17549, https://doi.org/10.1364/OE.23.017549.
[11] K. Wei, Z. Xu, R. Chen, X. Zheng, X. Cheng, T. Jiang, Temperature-dependent excitonic photoluminescence excited by two-photon absorption in perovskite CsPbBr_3 quantum dots, Opt. Lett. 41 (2016) 3821, https://doi.org/10.1364/OL.41.003821.
[12] J. Zhang, T. Jiang, T. Zhou, H. Ouyang, C. Zhang, Z. Xin, Z. Wang, X. Cheng, Saturated absorption of different layered Bi $_2$ Se $_3$ films in the resonance zone, Photon. Res. 6 (2018) C8, https://doi.org/10.1364/PRJ.6.0000C8.

[13] Y. Cui, X. Liu, Revelation of the birth and extinction dynamics of solitons in SWNT-mode-locked fiber lasers, Photon. Res. 7 (2019) 423, https://doi.org/10.1364/PRJ.7.000423.
[14] Y. Nakajima, Y. Hata, K. Minoshima, All-polarization-maintaining Er-fiber-based dual optical frequency combs with nonlinear amplifying loop mirror, in: CLEO Pacific Rim Conference, OSA, Hong Kong, 2018: p. F2A.6. doi: 10.1364/CLEOPR.2018.F2A.6.
[15] C. Zhao, J. Yao, H. Wang, Z. Tuo, E. Du, Y. He, Y. Meng, Research progress in optic frequency comb based on figue-of-9 mode-locking laser, Journal of Time, Frequency 45 (2022) 95–103, https://doi.org/10.13875/j.issn.1674-0637.2022-02-0095-09.
[16] J. Zhou, W. Pan, X. Fu, L. Zhang, Y. Feng, Environmentally-stable 50-fs pulse generation directly from an Er:fiber oscillator, Optical Fiber Technology 52 (2019) 101963, https://doi.org/10.1016/j.yofte.2019.101963.
[17] Y. Pengpeng, G. Hang, Y.e. Fei, C. Chaoliang, Lu. Wang Qingting, C.F. Shiyu, W. Tianye, L. Tingting, G. Zhengru, S. Xuling, Y. Kangwen, H. Qiang, Z. Heping, All Polarization-Maintaining Erbium-Doped Fiber Based Optical Comb, Chin. J. Laser 47 (2020) 0115001, https://doi.org/10.3788/CJL202047.0115001.
[18] Y. Zhou, Y. Zeng, J. Yin, T. Dong, L. Sun, Y. Zhang, K. Xu, All-polarization-maintaining figure-of-9 soliton and dispersion-managed Er-doped fiber oscillators, Laser Phys. 30 (2020) 045101, https://doi.org/10.1088/1555-6611/ab7a99.
[19] S. Lu, Q. Hao, T. Liu, F. Chen, X. Ren, X. Shen, M. Yan, H. Zeng, All Polarization Maintaining Fiber-Based Optical Comb System with Nonlinear Loop Mirror Mode-Locking, Chin. J. Laser 48 (2021) 2101002, https://doi.org/10.3788/CJL202148.2101002.
[20] N. Kuse, J. Jiang, C.-C. Lee, T.R. Schibli, M.E. Fermann, All polarization-maintaining Er fiber-based optical frequency combs with nonlinear amplifying loop mirror, Opt. Express 24 (2016) 3095, https://doi.org/10.1364/OE.24.003095.
[21] K. Yin, Y.-M. Li, Y.-B. Wang, X. Zheng, T. Jiang, Self-starting all-fiber PM Er:laser mode locked by a biased nonlinear amplifying loop mirror*, Chinese Phys. B 28 (2019) 124203, https://doi.org/10.1088/1674-1056/ab4d42.
[22] Q. Deng, K. Yin, J. Zhang, X. Zheng, T. Jiang, A 200 MHz Compact Environmentally-Stable Mode-Locked Figure-9 Fiber Laser, IEEE Photonics J. 13 (2021) 1–5, https://doi.org/10.1109/JPHOT.2021.3095159.
[23] H. Cheng, Z. Zhang, R. Pan, T. Zhang, Y. Feng, X. Hu, Y. Wang, S. Wu, Compact, repetition rate locked all-PM fiber femtosecond laser system based on low noise figure-9 Er:fiber laser, Optics & Laser Technology 158 (2023) 108818, https://doi.org/10.1016/j.optlastec.2022.108818.
[24] X. Cao, J. Zhou, Z. Cheng, S. Li, Y. Feng, GHz Figure-9 Er-Doped Optical Frequency Comb Based on Nested Fiber Ring Resonators, Laser & Photonics Reviews 17 (2023) 2300537, https://doi.org/10.1002/lpor.202300537.
[25] S. Xiong, D. Luo, Y. Liu, W. Wang, Z. Deng, Z. Tang, G. Xie, L. Zhou, Z. Zuo, C. Gu, W. Li, Investigation of stable pulse mode-locking regimes in a NALM figure-9 Er-doped fiber laser, Opt. Express 31 (2023) 514, https://doi.org/10.1364/OE.476630.
[26] W. Zhao, C. Yang, M. Shen, Enhanced Kelly sidebands of mode-locking fiber lasers for efficient terahertz signal generation, Optics & Laser Technology 137 (2021) 106802, https://doi.org/10.1016/j.optlastec.2020.106802.